

11-1-2012

Activation of protein kinase C δ leads to increased pancreatic acinar cell dedifferentiation in the absence of MIST1

Charis L. Johnson
Children's Health Research Institute, London, ON

Jodi M. Peat
Children's Health Research Institute, London, ON

Sonia N. Volante
Children's Health Research Institute, London, ON

Rennian Wang
Children's Health Research Institute, London, ON

Carolyn A. McLean
Western University

See next page for additional authors

Follow this and additional works at: <https://ir.lib.uwo.ca/paedpub>

Citation of this paper:

Johnson, Charis L.; Peat, Jodi M.; Volante, Sonia N.; Wang, Rennian; McLean, Carolyn A.; and Pin, Christopher L., "Activation of protein kinase C δ leads to increased pancreatic acinar cell dedifferentiation in the absence of MIST1" (2012). *Paediatrics Publications*. 1518.
<https://ir.lib.uwo.ca/paedpub/1518>

Authors

Charis L. Johnson, Jodi M. Peat, Sonia N. Volante, Rennian Wang, Carolyn A. McLean, and Christopher L. Pin

Activation of protein kinase C δ leads to increased pancreatic acinar cell dedifferentiation in the absence of MIST1

Charis L Johnson,^{1,2,3#} Jodi M Peat,^{1,2,3#} Sonia N Volante,^{1,2,3} Rennian Wang,^{1,3,5} Carolyn A McLean⁴ and Christopher L Pin^{1,2,3*}

¹ Children's Health Research Institute, London, ON, Canada

² Department of Paediatrics, University of Western Ontario, London, ON, Canada

³ Department of Physiology and Pharmacology, University of Western Ontario, London, ON, Canada

⁴ Department of Pathology, University of Western Ontario, London, ON, Canada

⁵ Department of Medicine, University of Western Ontario, London, ON, Canada

*Correspondence to: Christopher L Pin, Department of Paediatrics, University of Western Ontario, Children's Health Research Institute, 5th Floor, Victoria Research Laboratories, London, ON N6C 2V5, Canada. e-mail: cpin@uwo.ca

Co-first authors.

Abstract

Pancreatic ductal adenocarcinoma (PDAC) has a 5 year survival rate post-diagnosis of <5%. Individuals with chronic pancreatitis (CP) are 20-fold more likely to develop PDAC, making it a significant risk factor for PDAC. While the relationship for the increased susceptibility to PDAC is unknown, loss of the acinar cell phenotype is common to both pathologies. Pancreatic acinar cells can dedifferentiate or trans-differentiate into a number of cell types including duct cells, β cells, hepatocytes and adipocytes. Knowledge of the molecular pathways that regulate this plasticity should provide insight into PDAC and CP. MIST1 (encoded by *Bhlha15* in mice) is a transcription factor required for complete acinar cell maturation. The goal of this study was to examine the plasticity of acinar cells that do not express MIST1 (*Mist1*^{-/-}). The fate of acinar cells from C57Bl6 or congenic *Mist1*^{-/-} mice expressing an acinar specific, tamoxifen-inducible Cre recombinase mated to *Rosa26* reporter *LacZ* mice (*Mist1*^{CreERT/-} *R26r*) was determined following culture in a three-dimensional collagen matrix. *Mist1*^{CreERT/-} *R26r* acini showed increased acinar dedifferentiation, formation of ductal cysts and transient increases in PDX1 expression compared to wild-type acinar cells. Other progenitor cell markers, including *Foxa1*, *Sox9*, *Sca1* and *Hes1*, were elevated only in *Mist1*^{-/-} cultures. Analysis of protein kinase C (PKC) isoforms by western blot and immunofluorescence identified increased PKC ϵ accumulation and nuclear localization of PKC δ that correlated with increased duct formation. Treatment with rottlerin, a PKC δ -specific inhibitor, but not the PKC ϵ -specific antagonist ϵ V1-2, reduced acinar dedifferentiation, progenitor gene expression and ductal cyst formation. Immunocytochemistry on CP or PDAC tissue samples showed reduced MIST1 expression combined with increased nuclear PKC δ accumulation. These results suggest that the loss of MIST1 is a common event during PDAC and CP and events that affect MIST1 function and expression may increase susceptibility to these pathologies.

Copyright © 2012 Pathological Society of Great Britain and Ireland. Published by John Wiley & Sons, Ltd.

Keywords: pancreatitis; pancreatic ductal adenocarcinoma; MIST1; Bhlha15; protein kinase C; pancreatic and duodenal homeobox 1; trans-differentiation

Received 23 August 2011; Revised 14 February 2012; Accepted 22 February 2012

No conflicts of interest were declared.

Introduction

Pancreatic ductal adenocarcinoma (PDAC) is the fourth leading cause of cancer-related deaths in North America and treatment is complicated by the progressive nature of the disease at the time of diagnosis. Chronic pancreatitis (CP) also presents with significant morbidity and mortality, and individuals with CP are 20-fold more likely to develop PDAC, making it a significant risk factor for PDAC [1]. However, factors that promote increased PDAC susceptibility in CP have yet to be identified. Acinar cells exhibit significant plasticity through a process known as trans-differentiation [2,3] and dedifferentiation of acinar

cells to duct cells may be an initiating event in PDAC [4–6]. Acinar-to-duct cell trans-differentiation has been documented in human acini [7,8] and may potentially account for the increased predisposition of CP patients for PDAC [9]. Therefore, identification of factors that affect acinar cell plasticity is crucial.

In vivo, the development of pancreatic intra-epithelial neoplasia (PanIN) lesions occurred following over-expression of *Kras* in acinar cells [5,10]. In culture, epidermal growth factor, transforming growth factor- α and extracellular signal-regulated kinase (ERK)-1/2 all promote trans-differentiation of acinar cells [11–13]. While these studies highlight factors that increase acinar cell plasticity, complete understanding

of the process also requires identifying factors that prevent loss of the acinar cell phenotype.

MIST1 is a transcription factor expressed in exocrine-secreting cell types [14]. *Mist1* (*Bhlha15*) ablation in mice (*Mist1*^{-/-}) leads to incomplete acinar cell maturation, increased sensitivity to cerulein-induced pancreatitis (CIP) and altered expression of genes involved in cell communication and signalling [15–20]. In this context, MIST1's role appears to involve scaling-up the production of genes involved in regulated exocytosis [21]. MIST1 maintains the acinar cell phenotype as duct-like complexes believed to represent acinar-to-duct trans-differentiation events arise in aged or cultures *Mist1*^{-/-} pancreatic tissue [20,22,23]. The combined activation of *Kras* and loss of MIST1 in mice leads to development of ductal structures with little acinar cell differentiation and PDAC tumours are MIST1-negative [22]. These studies suggest that MIST1 is a key regulator of acinar cell plasticity.

The goals of this study were to examine the fate of acinar cells from *Mist1*^{-/-} mice *in vitro* or following injury, and identify the pathways that affect this fate. We found that *Mist1*^{-/-} acini activate progenitor gene expression and differentiate into duct cells. This process is dependent on activation of protein kinase C (PKC) δ . Changes in MIST1 expression and PKC δ localization observed during acinar cell dedifferentiation *in vivo* were also observed in PDAC and CP patient samples.

Methodology

Mice, tamoxifen injection and induction of pancreatitis

Procedures were approved by the University of Western Ontario Animal Care Committee (Protocol No. 2008-116). The mice used were in a C57B16 background. The mice containing a deletion of the *Mist1* gene (*Mist1*^{-/-}) or replacement with a tamoxifen-inducible Cre recombinase, heterozygous (*Mist1*^{creERT/+}) or homozygous (*Mist1*^{creERT/creERT}, referred to as *Mist1*^{creERT/-}), have been described [20,22]. *Mist1*^{creERT/+} mice were mated to *Rosa26* reporter mice (*R26r*) to generate mice for fate-mapping of acinar cells (*Mist1*^{creERT/+} *R26r*). Experimental pancreatitis was initiated as described [16]. Each mouse received eight intraperitoneal (i.p.) injections (50 μ g/kg) over 7 h. To induce Cre-mediated recombination, the mice were gavaged with 2 mg/kg tamoxifen, three times over 5 days. The mice were sacrificed 7 days later.

Reagents

All reagents were purchased from Fisher-Scientific (Nepean, ON, Canada), unless otherwise noted.

Isolation of primary acinar cells

Pancreata were dissected and acini isolated as described previously [24]. The acini were plated within a collagen matrix (VWR, Mississauga, ON, Canada) of a 1 : 1 solution of rat-tail collagen with Dulbecco's modified Eagle's medium (DMEM) containing 1% stock penicillin/streptomycin. Cultures were fed DMEM containing 1% penicillin/streptomycin (Pen/Strep), 0.25 μ g/ml amphotericin B, 0.1 mM IBMX and 1 μ M dexamethasone [25]. The medium was changed every 2 days unless stated. For pharmacological studies the medium was supplemented, starting on day 1 with Rottlerin (0.5–20 μ M), ϵ V1–2 (0.5–10 μ M), Bisindolylmaleimide I (Bis; 1–10 μ M) or PMA (10 nm–1 μ M). The cultures were followed for 9 days, with the medium refreshed daily. To assess cyst formation, the number of clusters containing cysts was determined from 50 randomly identified clusters. Treatments were performed in duplicate from at least three cultures established from independent mice.

Tissue isolation and histology

Mouse pancreata were fixed in formalin for paraffin embedding and sectioning, or fresh-frozen in cryomatrix and sectioned at 6 μ m. Cryostat sections were processed for X-gal histochemistry as described [14] or used for immunofluorescence (IF) (for antibody information, see Supporting information, Table S1). Acinar cells and collagen matrix were fixed in 4% formaldehyde overnight, then incubated in increasing sucrose concentrations, embedded in cryomatrix and sectioned. IF was performed as described [18] and visualized using a Leica upright microscope. Images were captured using the Openlab imaging system (Quorum Technologies, Guelph, ON, Canada).

Human tissue was obtained following guidelines established by the University of Western Ontario and the Lawson Health Research Institute, approved by the Research Ethics Board (REB) protocol #17012. Paraffin sections were obtained from patients diagnosed with CP ($n = 10$), PDAC ($n = 10$) or a non-related disease ($n = 10$; see Table 1). The slides were incubated for 30 min in 10 mM sodium citrate, pH 6, +0.05% Tween20 in a rice cooker, permeabilized for 10 min in phosphate-buffered saline (PBS) +0.1% Triton X and 7 min in 3% H₂O₂. The sections were blocked in 10% goat serum and then incubated sequentially in primary antibodies, biotinylated secondary antibodies and ABC reagent (Pierce, Rockford, IL, USA). 3,3'-Diamino benzidine was used as a chromagen. TUNEL analysis was performed following the manufacturer's instructions (*In Situ* Cell Death Detection Assay, Roche Diagnostics, Laval, PQ, Canada). In some cases, TUNEL was followed by IF for amylase.

Protein isolation and western blot analysis

Tissue protein extraction, protein electrophoresis and immunoblotting were performed as described [24].

Table 1. Summary of staining patterns observed in human samples for MIST1, PKC δ and PDX1

Patient [age (years), gender]	Diagnosis	Staining patterns		
		MIST1 ¹	PKC δ (acini) ²	PKC δ (lesions) ³
76, F	Gastric cancer	+, +++	–	+
58, F	Metastatic renal cell carcinoma	+++	–	+
55, M	Whipple procedure for non-pancreatic issues	+++	N	–
79, F	Whipple for inflammatory stricture of intrapancreatic common bile duct	+++	–	+
68, M	Gastric cancer	+, +++	–	–
48, M	Whipple procedure for lymphoma	+, +++	N	++
51, F	Whipple for VA of ampulla	++, +++	–	–
80, M	Whipple for TVA of ampulla; no pancreatitis	++, +++	–	++
72, M	Colon cancer	+, +++	–	++
55, M	Splenic lymphoma	++, +++	ND	ND
64.1 \pm 12.2 ⁴				
62, M	Chronic pancreatitis with pseudocyst	+, ++	–	++
48, M	Chronic pancreatitis with pseudocyst	+, +, +, +++	N	+
66, F	Chronic pancreatitis with pseudocyst	+, +++	N	+++
30, F	Chronic pancreatitis from gall stones	+	N	++
46, M	Chronic pancreatitis with pseudocyst	+	N	+
78, M	Chronic pancreatitis with pseudocyst; history of acute gallstone pancreatitis	+	–	+++
45, M	Chronic pancreatitis with pseudocyst	+	–	–
47, M	Chronic pancreatitis with pseudocyst	–	–	++
54, M	Chronic pancreatitis with pseudocyst, gall stone present	+, +, +, ++	N	+++
54, M	Chronic pancreatitis with pseudocyst; acute pancreatitis as well	+, +++	N	++
53 \pm 13.2 ⁴				
61, M	Pancreatic ductal adenocarcinoma	–, +	–	++
54, M	Pancreatic ductal adenocarcinoma	+, ++	N	++
64, M	Pancreatic ductal adenocarcinoma	–/+	–	++
73, F	Pancreatic ductal adenocarcinoma	+ / ++	–	++
61, F	Pancreatic ductal adenocarcinoma	–	–	+
54, M	Pancreatic ductal adenocarcinoma	–	–	+++
67, M	Pancreatic ductal adenocarcinoma	–/+	–	+++
75, M	Pancreatic ductal adenocarcinoma	– / ++	–	+
76, F	Pancreatic ductal adenocarcinoma	– / ++	–	+++
59, F	Pancreatic ductal adenocarcinoma	–	–	++
64.4 \pm 8.1 ⁴				

¹+, weak; ++, intermediate, +++, intense; –, no staining; when two staining patterns are apparent, both are provided. ²N, nuclear staining observed; –, no nuclear staining observed. ³+, <5% of the lesion area; ++, 5–50% of the lesion area; +++, >50% of the lesion area (showing nuclear PKC δ localization). ⁴Average age \pm SD. ND, not determined. VA, villous adenoma; TVA, tubulovillous adenoma.

RNA isolation and real-time qRT–PCR

RNA was isolated from cultures using TRIzol (Invitrogen, Burlington, ON, Canada), following the manufacturer's instructions. Quantitative (q) real-time RT–PCR was performed on cDNA samples prepared as described [24]. Using β -actin mRNA (*Actb*) as a normalization control, the CFX Manager 2.1 from Gene Study Analysis software (BioRad, Mississauga, ON, Canada) was used to calculate the amount of RNA relative to wild-type cultures obtained immediately, or 1 day, after isolation. Gene expression was calculated in the range 0–9 days in cultures or up to 5 days into treatment with rottlerin. Calculations for determining the relative abundance of each amplicon, primer sequences, annealing temperatures and amplicon sizes are listed in Table S2 (see Supporting information).

Statistical analysis

All values were compared by two-way ANOVA with a Bonferroni *post hoc* test, using Graph Pad Prism 5 (GraphPad Software, San Diego, CA, USA).

Results

To follow the fate of acinar cells in culture, the expression of amylase and pro-carboxypeptidase A (pCPA) was compared in wild-type (WT) and congenic *Mist1*^{–/–} pancreatic acini for up to 9 days following isolation. Western blot analysis revealed equal amounts of amylase and pCPA in WT and *Mist1*^{–/–} pancreatic protein extracts (Figure 1A). As previously observed, *Mist1*^{–/–} tissue contains active CPA, which appeared in WT and *Mist1*^{–/–} acinar cells upon culture. Both genotypes showed diminished accumulation of amylase and pCPA over time in culture. IF for amylase (Figure 1B) and CPA (Table 2; see also Supporting information, Figure S1A) was performed on cryostat sections of acini cultured for up to 5 days in collagen. One day into the culture, 89.1 \pm 3.2% of WT clusters and 79.7 \pm 4.7% of *Mist1*^{–/–} cell clusters were amylase-positive. CPA expression was found in 84.3 \pm 2.9% of WT clusters and 82.4 \pm 3.7% of *Mist1*^{–/–} clusters. By day 5,

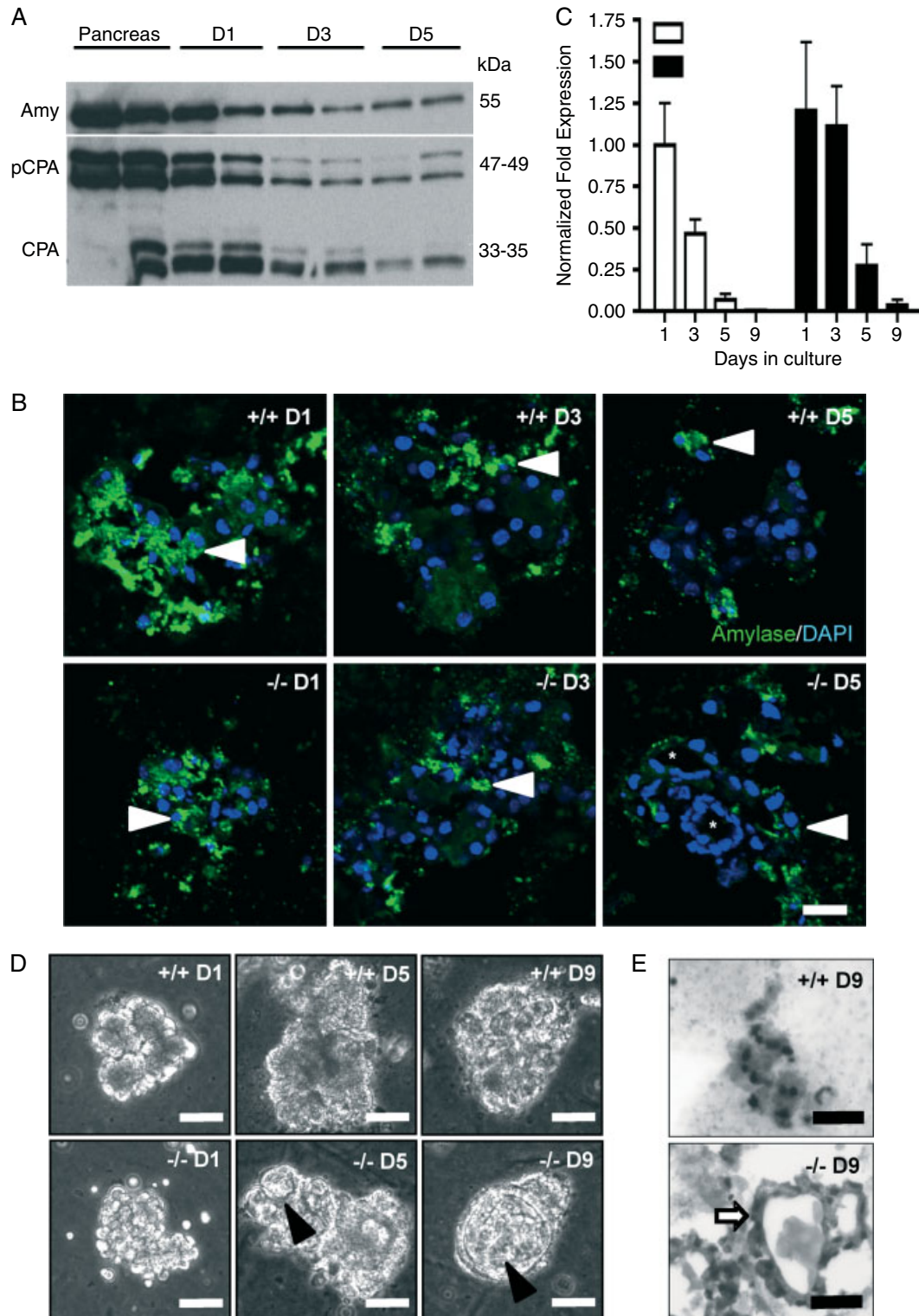


Figure 1. *Mist1*^{-/-} acinar cells exhibit a different morphological fate when compared to WT acini in culture. (A) Protein analysis by western blot reveals a rapid decrease in acinar cell gene expression upon culture. Amylase (Amy) and procarboxypeptidase (pCPA) are markedly decreased in both WT (+/+) and *Mist1*^{-/-} (-/-) cultures, while active carboxypeptidase (CPA) increased. (B) IF analysis for amylase on cryostat sections of acinar cells from WT (+/+) and *Mist1*^{-/-} (-/-) mice at 1 (D1), 3 (D3) and 5 (D5) days in culture; arrows indicate positive cells and cultures were co-labelled with DAPI to reveal nuclei; *tubular complexes observed in cross-section; bar = 15 μ m. (C) Relative accumulation of *amylase* RNA in WT (white bars) and *Mist1*^{-/-} (black bars) cultures up to 9 days after establishing cultures. Values are normalized to *Actb* and relative to WT *amylase* levels at day 1. Error bars represent mean \pm standard error(SE); * $p < 0.05$; ** $p < 0.01$, *** $p < 0.001$; $n = 5$. (D) Representative phase-contrast microscope images of WT or *Mist1*^{-/-} acini cultured for 1–9 days. Cysts (arrowheads) are observed in almost all *Mist1*^{-/-} acini by day 9. (E) haematoxylin and eosin (H&E) staining of sections derived from 9 day cultures reveal a flattened epithelium (arrow) surrounding a central lumen in *Mist1*^{-/-} cultures and pyknotic nuclei in wild-type cultures; bars = 40 μ m.

Table 2. Quantification of pancreatic differentiation markers by IF analysis

Marker	Expression within clusters (%)							
	Day 1		Day 3		Day 5		Day 7	
	WT	<i>Mist1</i> ^{-/-}	WT	<i>Mist1</i> ^{-/-}	WT	<i>Mist1</i> ^{-/-}	WT	<i>Mist1</i> ^{-/-}
Amylase	89.1 ± 3.2	79.7 ± 4.7	69.0 ± 6.6	52.6 ± 8.8	31.6 ± 5.7	19.2 ± 6.0	ND	ND
CPA	84.3 ± 2.9	82.4 ± 3.7	58.9 ± 4.3	48.7 ± 4.8	24.9 ± 3.2	16.1 ± 2.6	ND	ND
CK20	NI	NI	NI	NI	0.3 ± 0.3	0.2 ± 0.2	9.0 ± 3.5*	38.0 ± 6.4*
Insulin	0.3 ± 0.3	NI	0.3 ± 0.3	0.7 ± 0.4	NI	NI	ND	ND

NI, not identified; ND, not determined. All values are determined from $n = 3$, or $n = 2$ where noted*.

31.6 ± 5.7% of WT clusters expressed amylase, compared to 19.2 ± 6.0% of the *Mist1*^{-/-} clusters. At this time point, CPA was observed in 24.9 ± 3.3% of the WT clusters and in 16.1 ± 2.6% of *Mist1*^{-/-} cells. Therefore, it appears that a greater number of acinar cells lost their differentiated cell identity in the *Mist1*^{-/-} cultures. Interestingly, while qRT-PCR confirmed decreased *amylase* accumulation in culture, no differences were observed between *Mist1*^{-/-} and WT samples (Figure 1C).

IF revealed a number of clusters that contained flattened nuclei arranged in a circular fashion (* in Figure 1B). Examination of the morphology of acini by phase-contrast microscopy showed limited changes in WT cultures (Figure 1D). In contrast, *Mist1*^{-/-} acini underwent dramatic changes in morphology, developing cyst-like structures within 5 days. Acinar cell clusters were defined as containing a cyst when cells lining the cavity were obviously cuboidal or squamous in nature, as opposed to the columnar nature of acinar cells, and there was a lumen detectable by phase microscopy. By day 9, larger cysts could be observed in *Mist1*^{-/-} cultures, consisting of flattened epithelial cells (Figure 1E). Examination of individual clusters over several days confirmed that cysts developed over time in almost all (> 95%) *Mist1*^{-/-} clusters examined (see Supporting information, Figure S1B).

The loss of amylase-expressing cells could be the result of apoptosis, necrosis, degranulation or dedifferentiation of acinar cells. TUNEL analysis showed that 50% of the cells within *Mist1*^{-/-} cultures remained viable 11 days after establishing the cultures. At the same time, almost all WT cells were apoptotic (Figure 2A). Co-staining for amylase and TUNEL confirmed that many amylase cells were not apoptotic (Figure 2B), while TUNEL-positive cells were restricted mostly to non-cyst structures (Figure 2C). Analysis for HMGB1, a marker of necrotic cells [26], confirmed that few cells within the *Mist1*^{-/-} cultures were necrotic (see Supporting information, Figure S2). Co-IF for amylase and β -catenin indicated that most of the cells within the culture were epithelial in nature, exhibiting membrane localization of β -catenin indicative of adherens junctions (Figure 2D). The increase in amylase-negative cells were not the result of proliferation as IF for PCNA, Ki67 or phospho-histone 3, all markers of cell proliferation, labelled <1% of

the cells (data not shown). Additionally, cultures contained few CK20⁺ or insulin⁺ cells initially, suggesting that amylase-negative cells are derived from acinar cells (Table 2). By day 5, co-IF for amylase and CK20 identified CK20⁺ cells within *Mist1*^{-/-} cultures (Figure 2E). Few cells co-expressed amylase and CK20 but cysts containing both amylase⁺ and CK20⁺ cells were apparent (Figure 2E). Insulin⁺ cells were rarely observed. Interestingly, quantification of CK20⁺ cells 7 days into *Mist1*^{-/-} cultures revealed an increase to approximately 38 ± 6.4% of the total number of cells (Table 2). Therefore, it appears that *Mist1*^{-/-} acinar cells changed their differentiation characteristics in culture. We next assessed whether this change included dedifferentiation to a more progenitor-like state.

IF for the pancreatic progenitor cell marker, PDX1, revealed a robust, transient increase in PDX1 expression only in *Mist1*^{-/-} cultures (Figure 3A, B). No PDX1⁺ cells were observed in *Mist1*^{-/-} cultures immediately after isolation or at any time in WT cultures. Although co-IF for PDX1 and CK20 showed no co-localization within individual cells, cysts containing both PDX1⁺ and CK20⁺ cells were observed (Figure 3C). In some cases, IF for PDX1 showed non-nuclear localization. However, this staining was determined to be an artifact of the collagen cultures. Analysis for the progenitor cell marker *Scal* by qRT-PCR revealed a 200-fold increase in expression only in *Mist1*^{-/-} cultures (Figure 3D) that, similar to PDX1, was transient in nature.

Increased *Scal* expression suggests that *Mist1*^{-/-} acini may be dedifferentiating to non-pancreatic progenitor cells, and dexamethasone, which is part of the culture medium, can promote acinar-to-hepatocyte trans-differentiation [27,28]. Therefore, *Transferrin* and *ApoE* expression were assessed by qRT-PCR (Figure 3E, F). Both genotypes showed increased expression of *Transferrin*, an early marker of hepatocyte differentiation, but no expression of *ApoE*. However, the only point at which *Transferrin* levels were significantly higher in *Mist1*^{-/-} cultures was at day 9, at which point most WT acinar cells were dead. Interestingly, the contribution of hepatocytes to either culture was limited to <1% of all cells based on IF analysis (see Supporting information, Figure S3). Therefore, it does not appear that *Mist1*^{-/-} acinar cells have an increased ability for acinar-hepatocyte trans-differentiation compared to WT cultures.

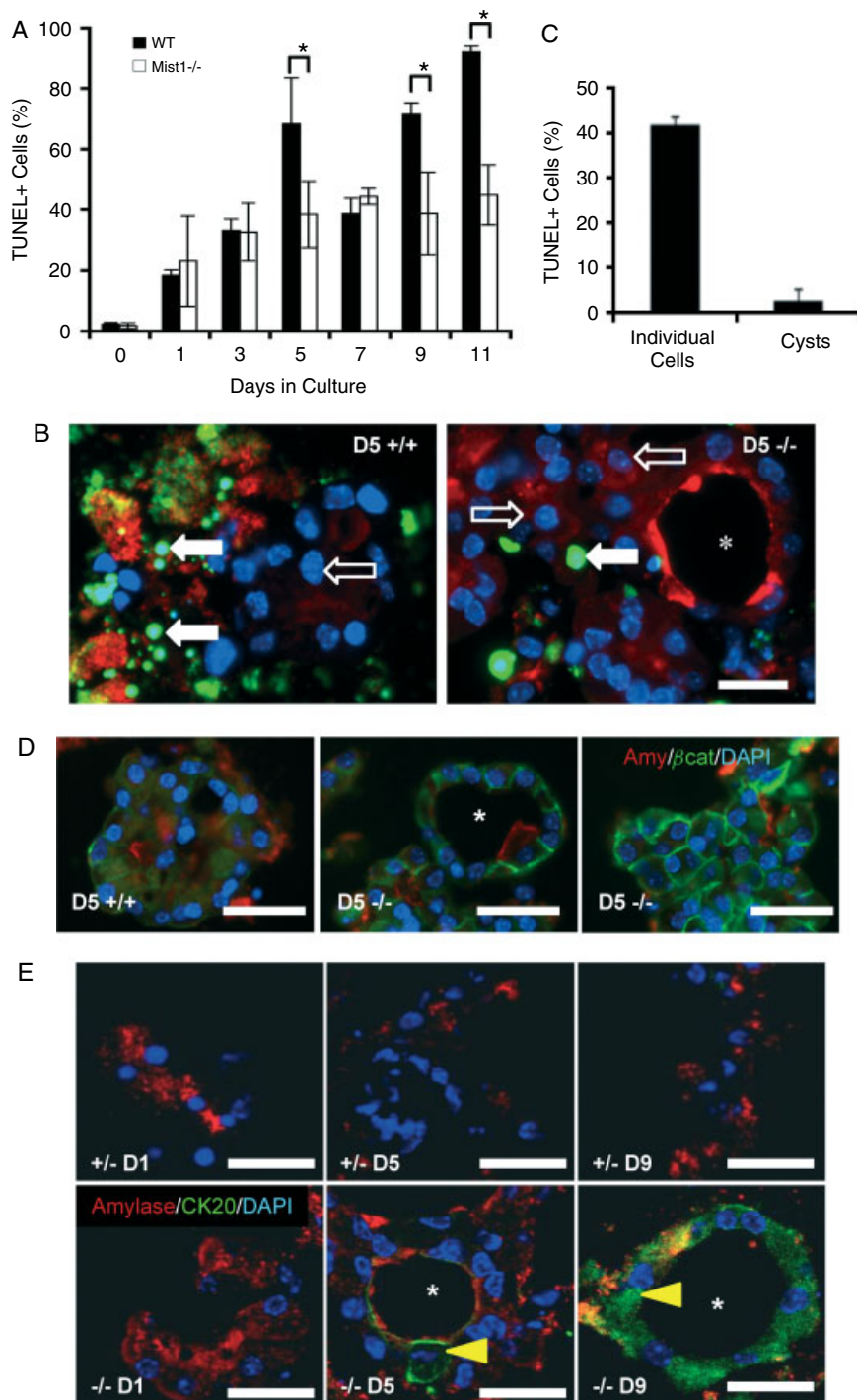


Figure 2. *Mist1*^{-/-} cysts show reduced apoptosis and characteristics of duct cells. (A) Quantitative analysis of apoptotic cells throughout time in culture based on TUNEL assays; $n = 3$ and $*p < 0.01$, using a two-way ANOVA and Bonferroni *post hoc* analysis. (B) Combined IF for amylase (red) and TUNEL (green) at day 5 in wild-type (+/+) or *Mist1*^{-/-} (-/-) cultures. Both apoptotic (filled arrow) and non-apoptotic (open arrow) amylase⁺ cells are observed. DAPI was used to stain nuclei (blue). *Cyst within *Mist1*^{-/-} cultures. (C) Quantification of the percentage of single cells or cells within cysts undergoing apoptosis in day 7 *Mist1*^{-/-} cultures; error bars represent mean \pm SE; $n = 3$, with at least 100 cells quantified for each condition. (D) Co-IF analysis for amylase (red) and β -catenin (green) in wild-type (+/+) or *Mist1*^{-/-} (-/-) acini cultured for 5 days (D5). (E) Co-IF analysis for amylase (red) and CK20 (green) in heterozygous (+/-) or *Mist1*^{-/-} (-/-) acini cultured for 1 (D1), 5 (D5) or 9 (D9) days; cysts (*) expressing CK20 are delineated by yellow arrows; bars = 20 μ m.

To be definitive that PDX1⁺ and CK20⁺ cell are derived from *Mist1*^{-/-} acinar cells, cultures were established from *Mist1*^{-/creERT} *R26r* mice, which harbour a tamoxifen-inducible Cre recombinase expressed from the *Mist1* locus (in the absence of MIST1 protein; [22]). After tamoxifen treatment, > 90% of all

acinar cells expressed β -galactoside (β -gal) with no evidence of β -gal expression in any ducts (Figure 4A). As previously reported [22], approximately 10% of islet cells stained positive for β -gal. Given the absence of insulin expression in the cultures, any *LacZ*⁺ cells observed in culture were deemed to be of acinar origin.

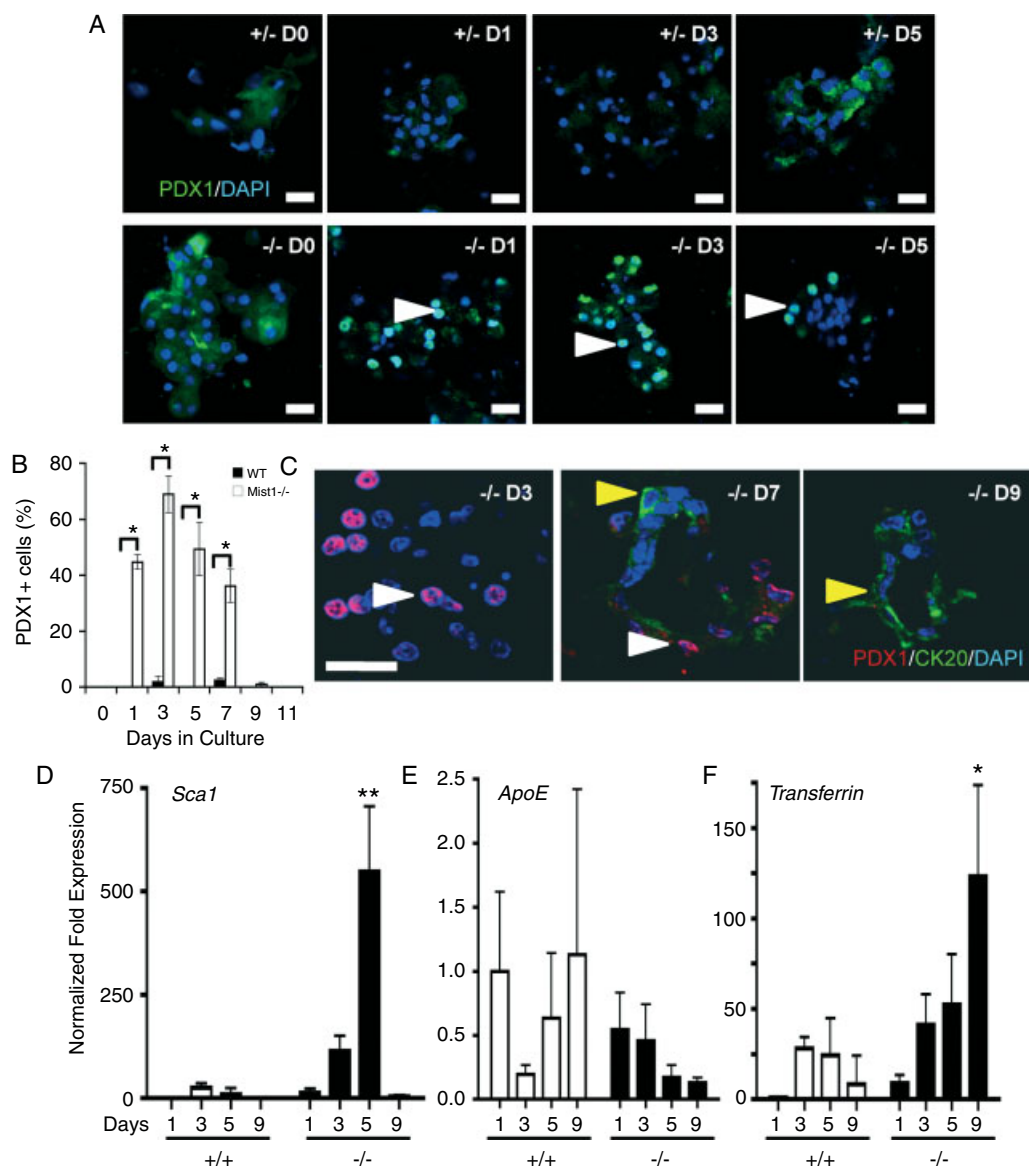


Figure 3. *Mist1*^{-/-} cultures express progenitor cell markers. (A) IF analysis for PDX1 reveals expression only in *Mist1*^{-/-} (-/-) and not heterozygote (+/-) cultures (arrows). (B) Quantification of the number of PDX1⁺ cells indicates extensive but transient PDX1 expression in *Mist1*^{-/-} cultures. $n = 3$; * $p < 0.01$. (C) Co-IF for CK20 (green, yellow arrow) and PDX1 (red, white arrow) identified acinar cell cultures that expressed both markers. However, in no instance was co-expression of the markers observed in the same cell. The cells were counterstained with DAPI; bar = 20 μm . (D–F) qRT-PCR for the progenitor cell marker *Sca1* (D), or early (*transferrin*; E) and late (*ApoE*; F) markers of hepatocyte differentiation. Values have been normalized to *Actb* and are relative to accumulation in WT cultures at day 1. Error bars represent mean \pm SE; two-way ANOVA was performed with Bonferroni *post hoc* test, and significance indicates differences between genotypes at the same time point; $n = 5$; * $p < 0.01$; ** $p < 0.001$.

Mist1^{-/creERT} *R26r* acini showed the same morphological chain of events observed in *Mist1*^{-/-} cultures, indicating that Cre recombinase did not affect cell differentiation. X-gal histochemistry and β -gal IF confirmed that 86% of cells in the culture were β -gal⁺, indicating that they were derived from acinar cells (Figure 4B). Counterstaining with haematoxylin showed X-gal⁺ cells with flattened nuclei adjacent to the cyst lumen (Figure 4C). Co-IF revealed a population of β -gal⁺/PDX1⁺ cells at days 1–5 in culture (Figure 4D, left panels) with fewer PDX1⁺ cells by day 7. Alternatively, co-IF revealed β -gal⁺/CK20⁺ cells at day 7 within the culture (Figure 4D, right panels). 30.2% and 75% of the cultured cells expressed

CK20 and β -gal, respectively, and 26% of the cells co-expressed both markers. These results confirm that *Mist1*^{-/-} acini give rise to progenitor and duct cells in culture.

We next asked whether pancreatic injury stimulates dedifferentiation *in vivo*. CIP resulted in the appearance of tubular structures in *Mist1*^{-/-} but not WT tissue within 8 h of initial injections (Figure 5A). 72 h post-initiation of CIP, widespread accumulation of X-gal⁺ tubular structures was observed throughout *Mist1*^{-/-} tissue (Figure 5B, C). Seven days after initiating CIP, tubular complexes were no longer apparent and the distribution of X-gal⁺ cells was once again restricted to acinar cells and a small proportion

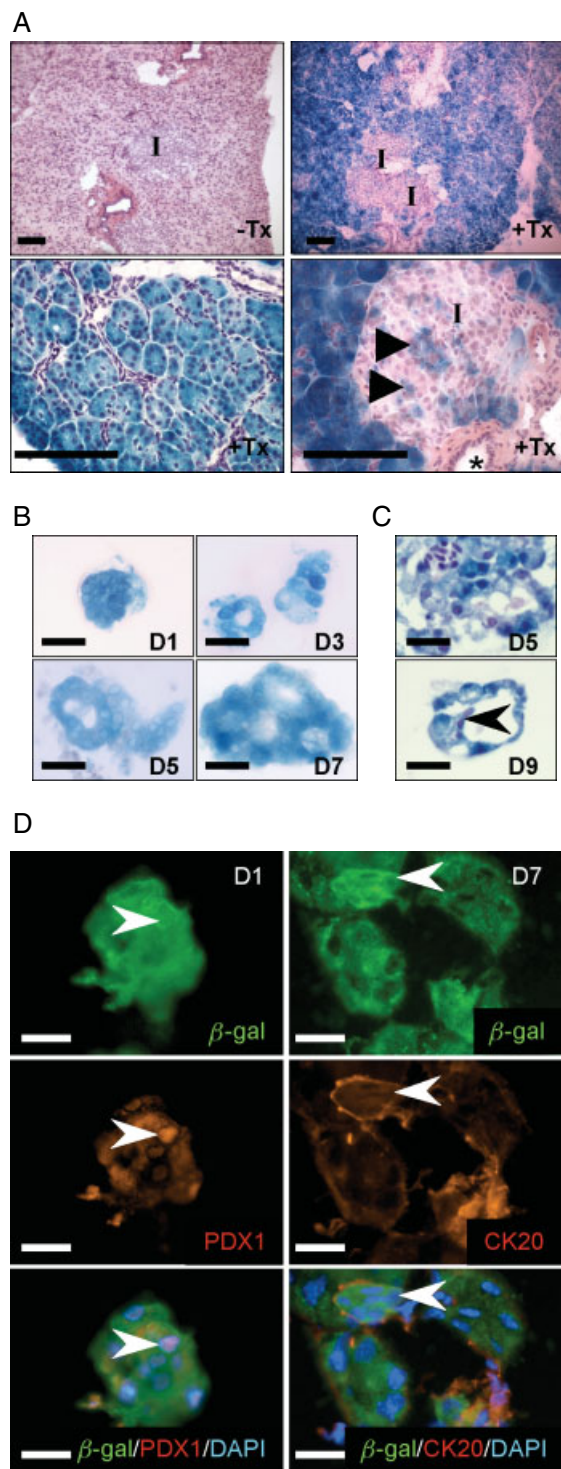


Figure 4. $PDX1^+$ and $CK20^+$ cells are derived from $Mist1^{-/-}$ acinar cells. (A) X-gal histochemistry combined with H&E staining shows specificity of *LacZ* expression following gavage without (-Tx) or with (+Tx) tamoxifen. Islets (I) show some X-gal⁺ cells, while acinar cells are almost uniformly positive and duct cells do not express X-gal; bar = 60 μ m. (B) X-gal histochemistry of $Mist1^{-/-}$ acini cultured for up to 7 days in culture. (C) X-gal histochemistry combined with haematoxylin staining revealed flattened epithelium expressing *LacZ* (arrow). Some cells do not stain for X-gal (arrowhead); bar = 30 μ m. (D) Co-IF for β -galactosidase (green) and either PDX1 or CK20 (red) in $Mist1^{-/-}$ acini cultured for 1 or 7 days. Co-expressing cells are delineated by arrows; cultures were counterstained with DAPI; bar = 15 μ m.

of islet cells, while duct cells were X-gal-negative (Figure 5C). It is possible that these tubular structures represent acinar cells undergoing degranulation. However, co-IF for PDX1 with β -gal or insulin revealed $PDX1^+/\beta$ -gal⁺ acinar cells in CIP-treated $Mist1^{-/-creERT}R26r$ tissue (Figure 5E). Saline-treated WT and $Mist1^{-/-creERT}R26r$ (Figure 5D) or CIP-treated WT showed PDX1 accumulation only within islets (see Supporting information, Figure S4). In some cases β -gal⁺/ $PDX1^-$ tubular complexes were observed, similar to that observed in culture. Whether these tubular complexes represent apoptotic acini or acinar cells undergoing complete trans-differentiation or redifferentiation into acinar cells is unclear.

To understand the signalling pathways that account for the conversion of $Mist1^{-/-}$ acini to duct-like cells, protein kinase C (PKC) signalling was examined. PKC signalling is key to acinar cell functions [29,30], and previous studies showed functional defects in $Mist1^{-/-}$ pancreata [15] that may be attributed to altered PKC signalling. Recent studies suggest that $PKC\delta$ can promote increased tumour growth of PANC1 cells *in vivo* [31]. Suppression of PKC signalling using the pan-PKC inhibitor Bis [32] reduced cyst formation in WT and $Mist1^{-/-}$ in a dose-dependent fashion (Figure 6A, B). Conversely, treatment of WT acinar cells with 100 μ M PMA, a PKC agonist [33], for 7 days resulted in $50.0 \pm 11.1\%$ of WT cell clusters developing cysts, compared to $18 \pm 7.5\%$ of the clusters in PBS-treated cultures (Figure 6C).

Analysis of PKC isoform expression by western blot revealed lower $PKC\alpha$ accumulation in $Mist1^{-/-}$ tissue, $PKC\delta$ expressed to equivalent levels in both genotypes and $PKC\epsilon$ and ζ expressed to higher amounts in $Mist1^{-/-}$ tissue (Figure 6D). Analysis of PKC localization by IF on sections from WT and $Mist1^{-/-}$ pancreatic tissue showed no difference in localization for $PKC\alpha$ and $PKC\zeta$ (see Supporting information, Figure S5), or $PKC\epsilon$ (Figure 6E) between WT and $Mist1^{-/-}$ tissue. Co-IF analysis of $PKC\delta$ and β -catenin revealed altered cellular $PKC\delta$ localization in the absence of *MIST1* (Figure 6F). $PKC\delta$ was expressed almost exclusively in the cytoplasm of WT acini with only minor nuclear localization. Conversely, the majority of $PKC\delta$ was localized to the nuclei of $Mist1^{-/-}$ acinar cells.

Due to the marked changes in $PKC\delta$ and $PKC\epsilon$ expression patterns, we treated cultures with isoform-specific inhibitors for $PKC\delta$ (rottlerin) or $PKC\epsilon$ (ϵ V1-2) [34–36]. A dose-dependent loss of cyst formation was found in rottlerin-treated WT and $Mist1^{-/-}$ cultures (Figure 7A, B; see also Supporting information, Figure S6), with no cysts observed at any time point upon incubation with 20 μ M rottlerin. Rottlerin treatment also abolished PDX1 accumulation (Figure 7E). Conversely, treatment with ϵ V1-2 resulted in increased cyst formation by 3 days in culture (Figure 7C, D). This effect was specific to $Mist1^{-/-}$ cultures suggesting that $PKC\epsilon$ may act in a compensatory mechanism to prevent acinar dedifferentiation. To determine whether

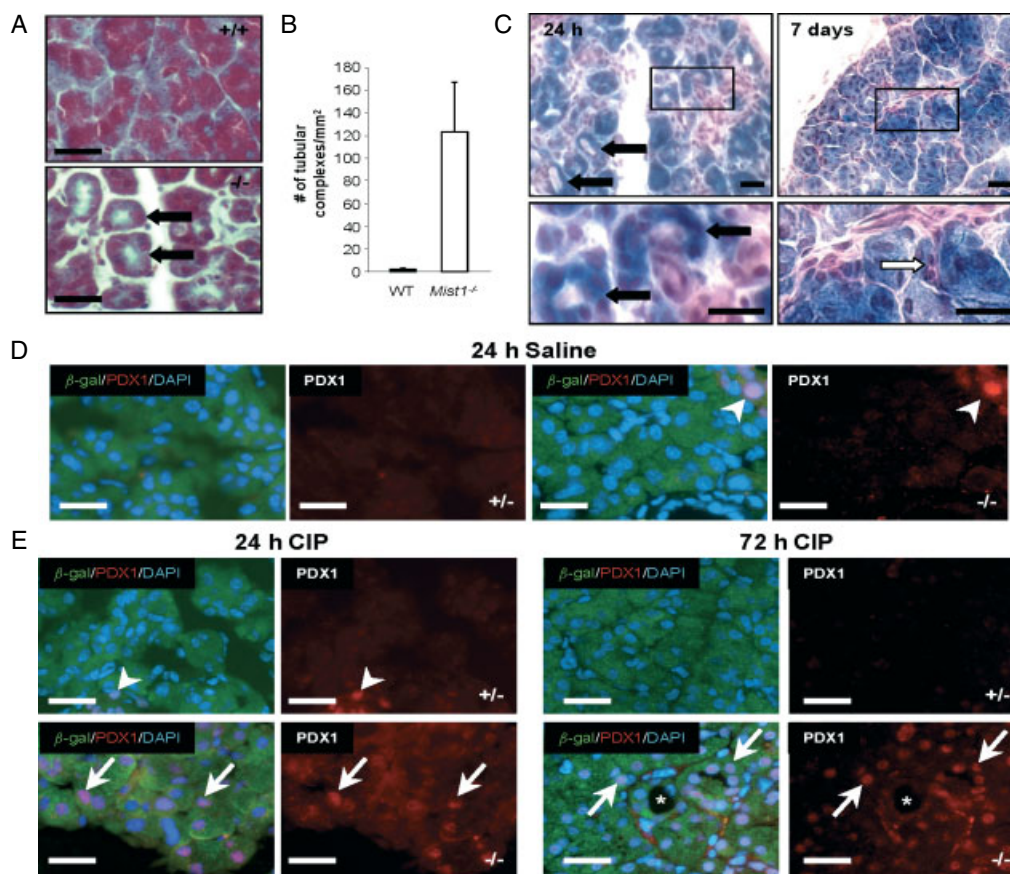


Figure 5. *Mist1*^{-/-} acinar cells give rise to tubular complexes and express PDX1 during CIP. (A) H&E analysis of pancreatic tissue sections from wild-type (+/+) or *Mist1*^{-/-} (-/-) mice, 24 h after initial cerulein injection revealed tubular complexes (arrows); bars = 40 μm. (B) Quantification of tubular complexes in wild-type and *Mist1*^{-/-} tissue 72 h after initial cerulein injections. (C) H&E staining was combined with X-gal histochemistry on pancreatic sections from *Mist1*^{-/-} mice. 24 h after initiating pancreatitis, tubular complexes that are X-gal-positive (arrows) are easily observed. By 7 days after initiating CIP, all duct cells (white arrow) are X-gal-negative, while the majority of acinar cells are X-gal-positive; bars = 25 μm. (D, E) Co-IF for β-gal and PDX1 on pancreatic sections from saline or cerulein (CIP)-treated wild-type (+/+) or *Mist1*^{-/-} (-/-) mice, 24 or 72 h after initial injection. PDX1 expression is limited to islets (arrowheads) in saline-treated *Mist1*^{-/-} tissue and all wild-type tissue. CIP-treated *Mist1*^{-/-} acinar cells show extensive expression of PDX1, including some tubular complexes (arrows). Some tubular complexes were also found to be negative for PDX1 expression (*); bars = 30 μm.

blocking PKCδ affected the transcriptional profile of *Mist1*^{-/-} cultures, qRT-PCR was used to compare gene expression 1 and 5 days after treatment with PBS or 1 and 10 μM rottlerin (Figure 7F, G). PBS-treated *Mist1*^{-/-} cultures showed significantly higher levels of *Pdx1* and *Sca1* compared to WT cultures, as well as elevated levels of progenitor markers *Foxa1*, *Hes1* and *Sox9*. With the exception of *Sox9*, progenitor gene expression was significantly reduced in rottlerin-treated cultures. Blocking PKCδ activity also significantly reduced *Krt19* (cytokeratin 19, marker of duct cells) expression, but not *Transferrin*, suggesting that PKCδ may specifically promote dedifferentiation to pancreatic progenitor cells.

Finally, we examined MIST1, PKCδ and PDX1 localization in pancreatic tissue obtained from patients with CP, PDAC or non-pancreatic malignancies (Table 1, Figure 8). MIST1 expression was observed in all control samples ($n = 10$, Figure 8A). Reduced MIST1 accumulation was observed in CP and PDAC tissues with several CP (5/10) and PDAC (6/10) samples containing extensive areas of MIST1-negative

tissue. MIST1 was also absent in PanIN lesions, as previously described (see Supporting information, Figure S7) [22]. Nuclear localization of PKCδ in acinar cells was observed in a few control (2/9) and PDAC (1/10) samples, but was readily apparent in CP samples (6/10) (Figure 8A). Nuclear PKCδ localization increased in tubular complexes found within normal (6/9) and CP (9/10) samples and was observed in low- (Figure 8C) and high-grade (Figure 8D) PanIN lesions for all PDAC samples (10/10). Increased nuclear PKCδ localization correlated with increased expression of PDX1 in non-islet tissue (Figure 8A–D), although PDX1 did not always correlate with areas of PKCδ staining.

Discussion

Evidence in mouse models and human pancreatic disease supports acinar cell dedifferentiation as a factor contributing to pancreatic disease [7,37]. In this study, we showed that the absence of MIST1 increased acinar cell dedifferentiation *in vitro*, dependent on PKCδ

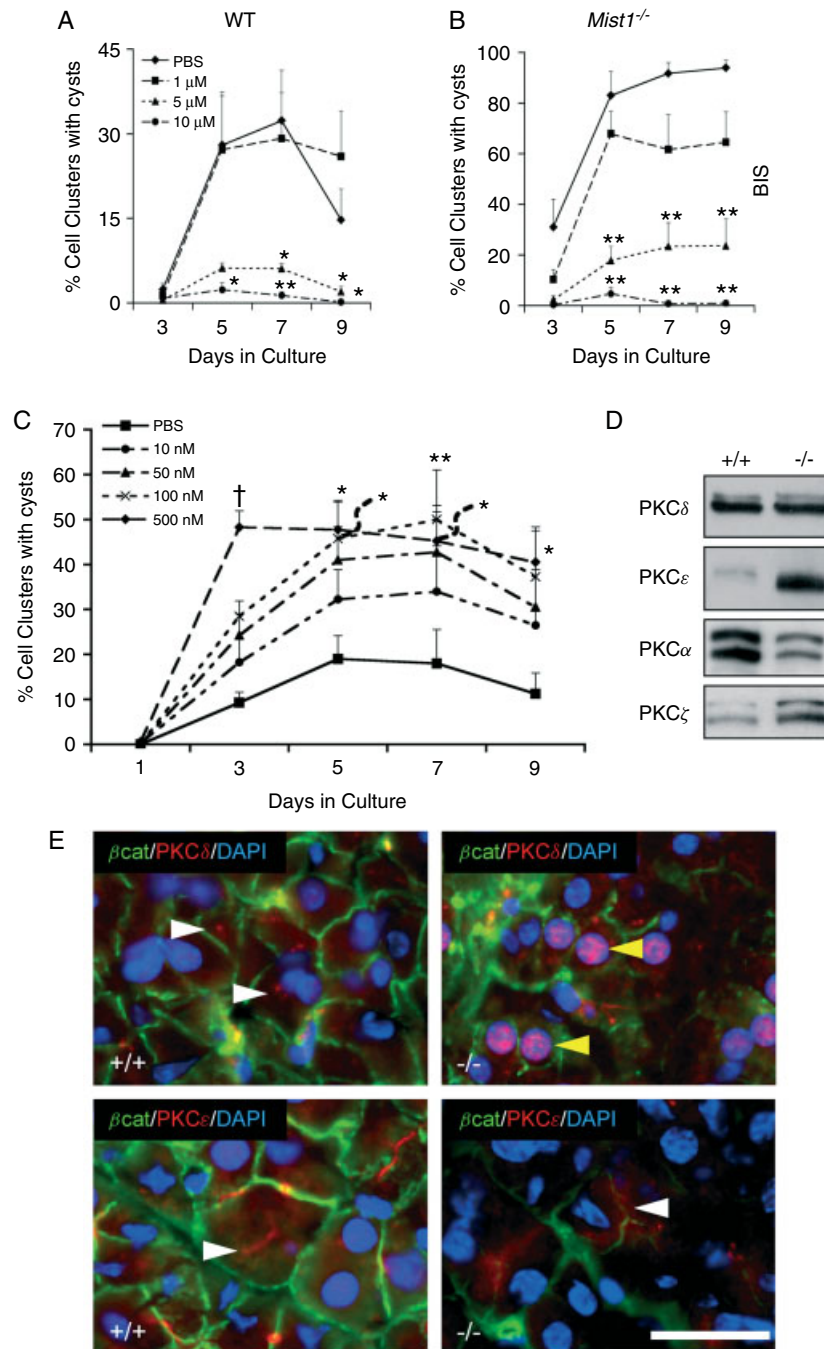


Figure 6. PKC activity affects cyst formation of acinar cells. Quantification of the percentage of acinar cell clusters containing cysts in (A) wild-type and (B) *Mist1*^{-/-} cultures incubated in PBS or with 1–10 μ M bisindolylmaleimide I, a Pan-PKC inhibitor, or (C) in WT cultures incubated in 10–500 nM PMA, a PKC agonist; * p < 0.05; ** p < 0.01; † p < 0.001 relative to PBS control-treated samples. (D) Western blot analysis for PKC δ , ϵ , α and ζ expressed in whole pancreatic tissue extracts from wild-type or *Mist1*^{-/-} mice. (E) Representative co-IF for PKC ϵ or PKC δ (red) combined with β -catenin (green) in WT (+/+) or *Mist1*^{-/-} (-/-) pancreatic tissue sections from 2 month-old mice. White arrowheads indicate cytoplasmic localization of each PKC isoform, and yellow arrowheads indicate nuclear localization of PKC δ only in *Mist1*^{-/-} acinar cells; bar = 20 μ m.

activity. We also showed that decreased MIST1 expression, and localization of PKC δ to the acinar nucleus, occurs in patients with PDAC and CP. Therefore, events that affect MIST1 and PKC δ function will have consequences on the differentiation status of acinar cells and susceptibility to disease.

MIST1 is a transcription factor required for acinar cell maturation, organization and function [20]. To date, identified targets of MIST1's transcriptional activity

include *Gjb1*, *Rab3d*, *Rab26* and *Atp2c2* [15,18,19,38] and a recent model suggests that MIST1 acts as a scaling factor to promote exocytosis [21]. Our results support a role for MIST1 in maintaining a mature phenotype. In the absence of MIST1, acinar cells are more susceptible to K-ras activation. A complete absence of MIST1 in the presence of active Kras resulted in large tubular structures developing in neonatal mice in place of normal acinar tissue [22]. The current

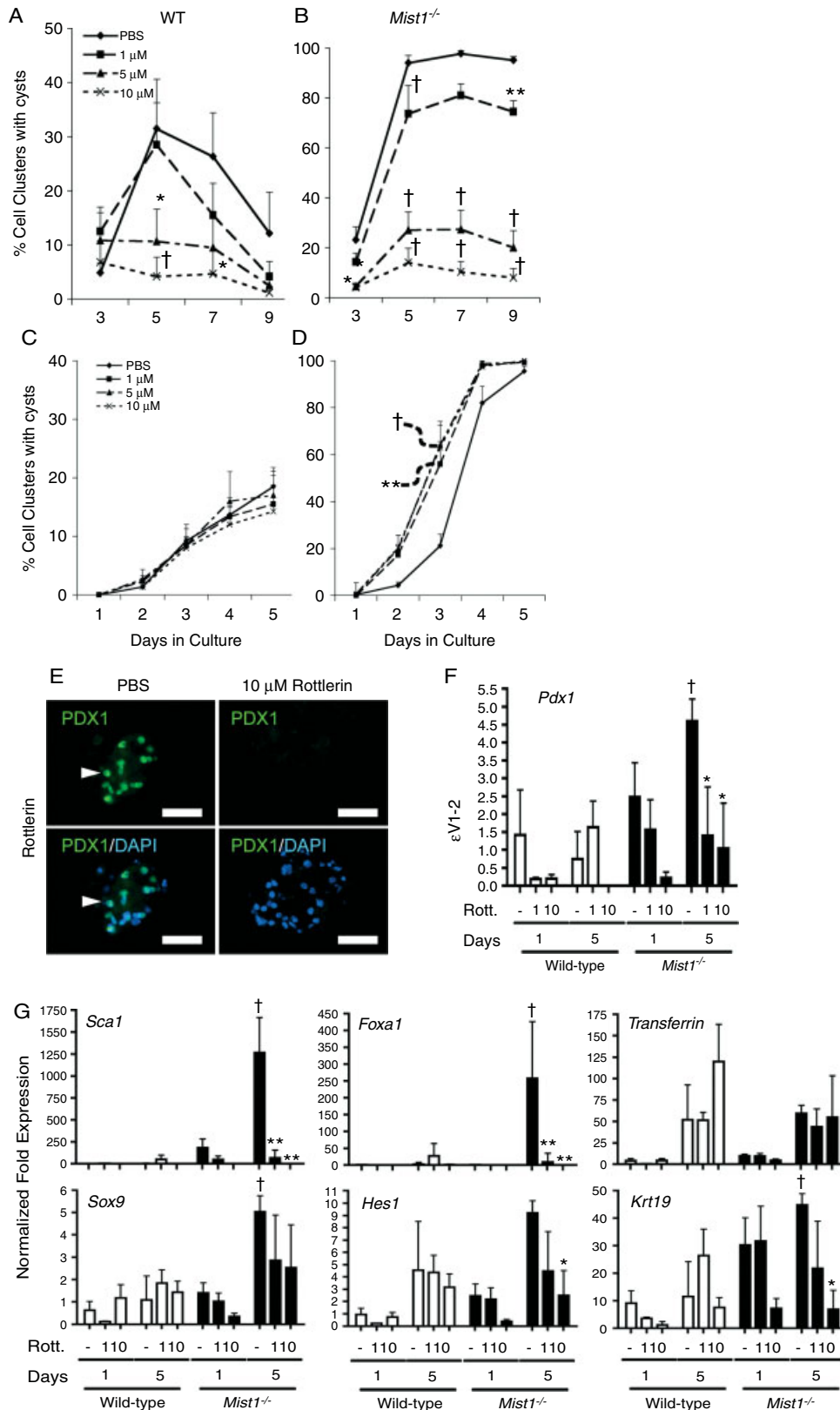


Figure 7. Specific inhibition of PKC δ blocks cyst formation and PDX1 expression in *Mist1*^{-/-} acinar cells. Quantification of the percentage of acinar cell clusters that develop cysts following incubation of (A, C) WT and (B, D) *Mist1*^{-/-} acinar cells in (A, B) 500 nM–20 μ M rottlerin (PKC δ inhibitor) or (C, D) 500 nM–10 μ M eV1-2 (PKC ϵ inhibitor); **p* < 0.05; ***p* < 0.01; †*p* < 0.001 relative to PBS control-treated samples; in (D) † refers to both 5 and 10 μ M treatments. (E) IF for PDX1 in *Mist1*^{-/-} cultures following 5 days of treatment with PBS or 10 μ M rottlerin; cultures were co-stained with DAPI; bar = 50 μ m. qRT-PCR for (F) *Pdx1* or (G) markers of progenitor cells (*Sca1*, *Foxa1*, *Sox9* and *Hes1*), hepatocytes (*Transferrin*) and duct cells (*Krt19*; cytokeratin 19), comparing RNA accumulation in WT and *Mist1*^{-/-} cultures treated with PBS or 1 or 10 μ M rottlerin for 1 or 5 days. All values were normalized to *Actb* and relative to transcript levels in WT cultures immediately after isolation. Significant differences are observed between WT and *Mist1*^{-/-} cultures (indicated by †*p* < 0.001) or between *Mist1*^{-/-} cultures treated with PBS or rottlerin (indicated by **p* < 0.05 or ***p* < 0.01); error bars represent mean \pm SE; *n* = 5.

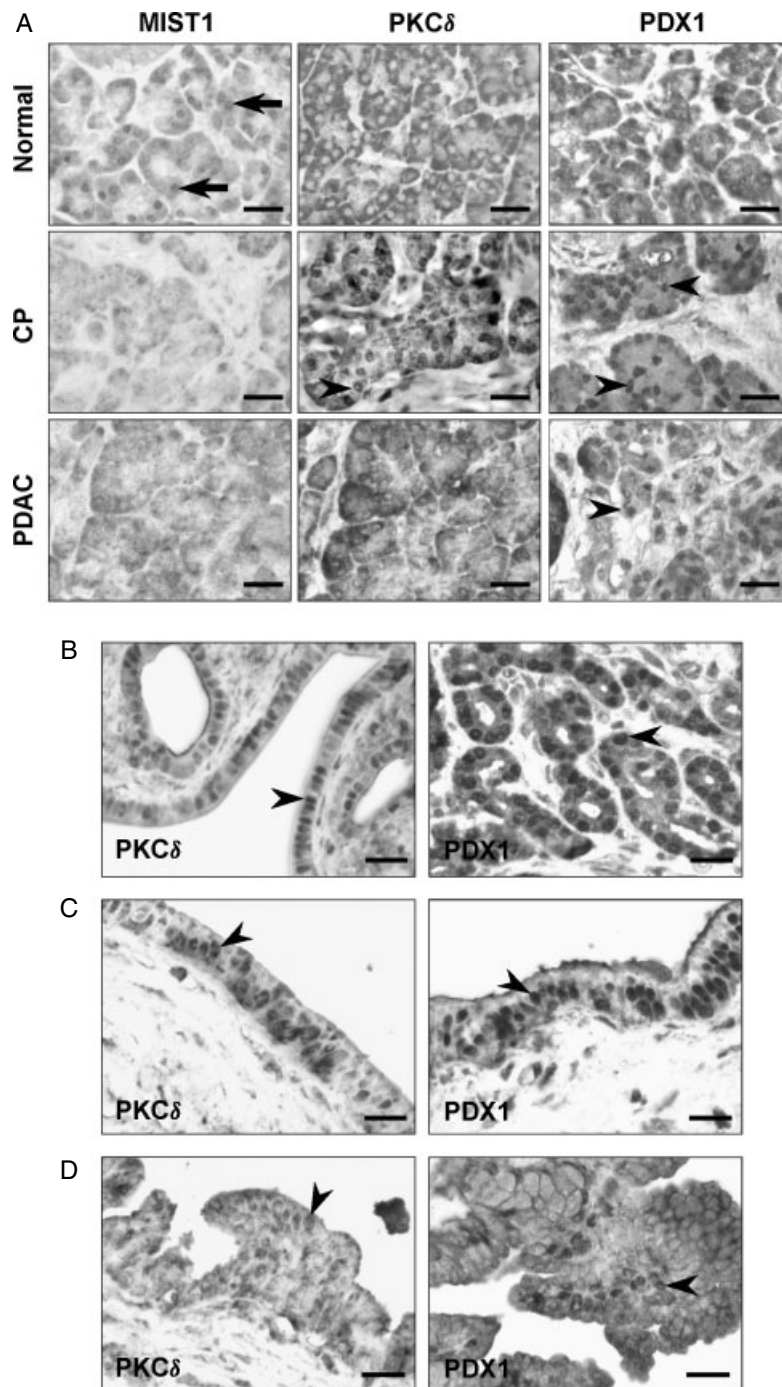


Figure 8. MIST1 accumulation decreases and nuclear localization of PKC δ increases in pancreatic tissue from CP and PDAC patients. (A) IHC analysis of MIST1, PKC δ or PDX1 expression in acinar tissue from control pancreatic tissue, or tissue from patients with chronic pancreatitis (CP) or pancreatic ductal adenocarcinoma (PDAC). Arrows indicate MIST1 expression in normal tissue that is decreased or lost in CP and PDAC samples, respectively. Arrowheads indicate nuclear localization of PKC δ and PDX1. IHC for PKC δ or PDX1 in (B) duct complexes from CP samples, or from (C) low- and (D) high-grade PanIN lesions; arrowheads indicate nuclear localization; bars = 30 μ M.

study shows that in the absence of constitutively active Kras, the response of *Mist1*^{-/-} acini to injurious stimulation, through culture or induction of pancreatitis, was dramatically different than WT acinar cells. *Mist1*^{-/-} acini re-expressed a number of pancreatic (*Pdx1*, *Hes1* and *Sox9*) and general (*Foxa1* and *Sca1*) progenitor cell markers [39–43]. It could be argued that *Mist1*^{-/-} cultures contained progenitor cells not found in WT cultures; however, lineage tracing revealed

PDX1⁺ cells co-expressing β -gal, and the percentage of PDX1⁺ cells increased dramatically at a time when limited cell proliferation was observed within the cultures (data not shown). It is interesting that no increase in PDX1 expression was observed during CIP in WT mice. However, increased and decreased PDX1 expression has been documented in CIP [44,45]. Therefore, differences in PDX1 expression may be due to the experimental model, reflecting differences in

cerulein dosing or the genetic background of the mice. The fact that our WT mice showed very limited damage and no tubular complexes may speak to this difference.

A previous study examined MIST1 expression in PDAC, showing increased cyst formation in *Mist1*^{-/-} cultures [21]. However, the work presented here is the first study to assess MIST1 protein expression in human CP tissue, and showed a consistent decrease in acinar cell MIST1 expression. In addition, our study showed decreased MIST1 expression in acinar tissue adjacent to tumours in PDAC, unlike studies on MIST1 expression in PDAC and carcinomas of stomach epithelium [22,46], where MIST1 expression was maintained in differentiated cells. The difference in our results compared to previous work may be due to the tissue samples assessed. MIST1 expression was maintained in small pockets of acini in PDAC samples, suggesting heterogeneity to the disease. However, MIST1-negative acinar tissue in the majority of PDAC samples (8/10) suggests that decreases in MIST1 may contribute to cancer progression. Similar decreases in MIST1 in CP samples provide another link between CP and the increased susceptibility for PDAC. Therefore, defects in MIST1 expression and function may be potential markers of susceptibility for CP and PDAC. These findings suggest that the loss of MIST1 precedes development of PDAC, however; the loss of MIST1 may reflect non-cell autonomous influences from the tumours on acinar cell biology. For instance, local factors within the tissue, such as increased stroma or inflammation, could alter MIST1 expression. Delineating whether the loss of MIST1 contributes to, or is a product of, the development of PDAC is a critical question moving forward in understanding its pathology.

Finally, our study greatly expanded on previous work showing that trans-differentiation of *Mist1*^{-/-} acini first involves dedifferentiation to a progenitor cell type, and implicates PKC δ in acinar dedifferentiation by identifying a unique relationship between PKC signalling and progenitor cell gene expression. Inhibition of PKC δ abolished acinar dedifferentiation, based on decreased cyst formation and progenitor cell gene expression, while treatment of WT cultures with PMA markedly increased cyst formation, indicating that PKC δ can promote acinar cell dedifferentiation and was not unique to the *Mist1*^{-/-} phenotype. Bis, which inhibits classical (PKC α) and novel PKC (PKC δ , PKC ϵ) isoforms [32], also inhibited cyst formation, while PKC ϵ -specific inhibitors did not, supporting a role for PKC δ in acinar dedifferentiation. Interestingly, inhibition of PKC δ did not affect expression of the liver-specific marker, *Transferrin*, suggesting that PKC δ is not involved in acinar–hepatocyte trans-differentiation.

Normally, PKC δ is required for regulated exocytosis in response to secretagogue stimulation [30,47]. While recent studies have shown that increased proliferation and tumour formation occurs in PKC δ -expressing PANC1 cells [31], cell localization was not assessed.

Our analysis identified specific PKC δ nuclear localization in acinar cells of CP tissue and PanINs. Nuclear localization of PKC δ has been linked to both increased and decreased apoptosis [48–51]. However, since the isoform of PKC δ that prevents apoptosis is believed to be a dominant negative regulator of PKC δ signalling [48], it is unclear whether nuclear localization of PKC δ in acinar cells drives the process of acinar dedifferentiation or is unrelated to this event.

The simplest model suggests that MIST1 represses PKC δ to prevent dedifferentiation. However, a rapid decrease in MIST1 accumulation occurs within 24 h of isolating acinar cells (data not shown), and microarray analysis indicated that *PKC δ* mRNA levels did not change in *Mist1*^{-/-} pancreatic tissue [16]. An alternative explanation is that *Mist1*^{-/-} acinar cells have adapted to a cell environment that includes premature enzyme activation and cellular disorganization. We observed alterations in the ER stress-response pathway during CIP or following ethanol feeding, suggesting adaptation [16,52], and the increased PKC ϵ accumulation in *Mist1*^{-/-} tissue may be part of an adaptive response. Inhibiting PKC ϵ activity enhanced dedifferentiation, and CIP or culture may provide a tipping point by which PKC ϵ no longer inhibits dedifferentiation. Antagonism between PKC ϵ and δ occurs in other systems, such as cardiac hypertrophy [53].

In conclusion, we have identified MIST1 as a repressor of acinar cell dedifferentiation and a possible diagnostic marker for exocrine pancreatic diseases. The absence of MIST1 may provide the link between CP and PDAC, as its absence increases the ability for acini to convert to duct cells.

Acknowledgment

The authors would like to thank Dr Stephen Konieczny for supplying *Mist1*^{-/CreERT} *R26r* and critically evaluating the manuscript. We would also like to thank Dr Agnes Kowalik for technical aspects related to the work. This work was funded by operating grants from the Canadian Institutes of Health Research (CIHR; Grant No. CP-MOP53083), the Children's Health Research Institute and the Lawson Health Research Institute, and would not have been possible without the support of the Children's Health Foundation. Finally, we would like to acknowledge Dr Gabriel DiMattia, Dr Tom Drysdale, Elena Fazio and Dr Rashid Mehmood for their input into the study.

Author contributions

CLJ and JMP, acquisition, analysis and interpretation of data, drafting of the manuscript and statistical analysis; SNV, acquisition of data and statistical analysis; CAM and RW, technical support and critical revision for important intellectual content; CLP, study concept

and design, analysis and interpretation of data, critical revision for important intellectual content, statistical analysis, obtaining funding and study supervision.

References

- Krejs GJ. Pancreatic cancer: epidemiology and risk factors. *Dig Dis* 2010; **28**: 355–358.
- Lardon J, De Breuck S, Rooman I, et al. Plasticity in the adult rat pancreas: transdifferentiation of exocrine to hepatocyte-like cells in primary culture. *Hepatology* 2004; **39**: 1499–1507.
- Slack JM. Metaplasia and transdifferentiation: from pure biology to the clinic. *Nat Rev Mol Cell Biol* 2007; **8**: 369–378.
- Shi C, Hong SM, Lim P, et al. KRAS2 mutations in human pancreatic acinar-ductal metaplastic lesions are limited to those with PanIN: implications for the human pancreatic cancer cell of origin. *Mol Cancer Res* 2009; **7**: 230–236.
- Habbe N, Shi G, Meguid RA, et al. Spontaneous induction of murine pancreatic intraepithelial neoplasia (mPanIN) by acinar cell targeting of oncogenic Kras in adult mice. *Proc Natl Acad Sci USA* 2008; **105**: 18913–18918.
- De La OJ, Emerson LL, Goodman JL, et al. Notch and Kras reprogram pancreatic acinar cells to ductal intraepithelial neoplasia. *Proc Natl Acad Sci USA* 2008; **105**: 18907–18912.
- Houbracken I, de Waele E, Lardon J, et al. Lineage tracing evidence for transdifferentiation of acinar to duct cells and plasticity of human pancreas. *Gastroenterology* 2011; **141**: ; e734 731–741.
- Hall PA, Lemoine NR. Rapid acinar to ductal transdifferentiation in cultured human exocrine pancreas. *J Pathol* 1992; **166**: 97–103.
- Puri S, Hebrok M. Cellular plasticity within the pancreas—lessons learned from development. *Dev Cell* 2010; **18**: 342–356.
- Tuveson DA, Zhu L, Gopinathan A, et al. *Mist1*–*KrasG12D* knock-in mice develop mixed differentiation metastatic exocrine pancreatic carcinoma and hepatocellular carcinoma. *Cancer Res* 2006; **66**: 242–247.
- Baeyens L, De Breuck S, Lardon J, et al. *In vitro* generation of insulin-producing β cells from adult exocrine pancreatic cells. *Diabetologia* 2005; **48**: 49–57.
- Minami K, Okuno M, Miyawaki K, et al. Lineage tracing and characterization of insulin-secreting cells generated from adult pancreatic acinar cells. *Proc Natl Acad Sci USA* 2005; **102**: 15116–15121.
- Means AL, Meszoely IM, Suzuki K, et al. Pancreatic epithelial plasticity mediated by acinar cell transdifferentiation and generation of nestin-positive intermediates. *Development* 2005; **132**: 3767–3776.
- Pin CL, Bonvissuto AC, Konieczny SF. *Mist1* expression is a common link among serous exocrine cells exhibiting regulated exocytosis. *Anat Rec* 2000; **259**: 157–167.
- Garside VC, Kowalik AS, Johnson CL, et al. *MIST1* regulates the pancreatic acinar cell expression of *Atp2c2*, the gene encoding secretory pathway calcium ATPase 2. *Exp Cell Res* 2010; **316**: 2859–2870.
- Kowalik AS, Johnson CL, Chadi SA, et al. Mice lacking the transcription factor *Mist1* exhibit an altered stress response and increased sensitivity to caerulein-induced pancreatitis. *Am J Physiol Gastrointest Liver Physiol* 2007; **292**: G1123–1132.
- Luo X, Shin DM, Wang X, et al. Aberrant localization of intracellular organelles, Ca^{2+} signaling, and exocytosis in *Mist1* null mice. *J Biol Chem* 2005; **280**: 12668–12675.
- Johnson CL, Kowalik AS, Rajakumar N, et al. *Mist1* is necessary for the establishment of granule organization in serous exocrine cells of the gastrointestinal tract. *Mech Dev* 2004; **121**: 261–272.
- Rukstalis JM, Kowalik A, Zhu L, et al. Exocrine specific expression of Connexin 32 is dependent on the basic helix–loop–helix transcription factor *Mist1*. *J Cell Sci* 2003; **116**: 3315–3325.
- Pin CL, Rukstalis JM, Johnson C, et al. The bHLH transcription factor *Mist1* is required to maintain exocrine pancreas cell organization and acinar cell identity. *J Cell Biol* 2001; **155**: 519–530.
- Mills JC, Taghert PH. Scaling factors: transcription factors regulating subcellular domains. *Bioessays* 2011; **34**: 10–16.
- Shi G, Zhu L, Sun Y, et al. Loss of the acinar-restricted transcription factor *Mist1* accelerates *Kras*-induced pancreatic intraepithelial neoplasia. *Gastroenterology* 2009; **136**: 1368–1378.
- Zhu L, Tran T, Rukstalis JM, et al. Inhibition of *Mist1* homodimer formation induces pancreatic acinar-to-ductal metaplasia. *Mol Cell Biol* 2004; **24**: 2673–2681.
- Johnson CL, Weston JY, Chadi SA, et al. Fibroblast growth factor 21 reduces the severity of cerulein-induced pancreatitis in mice. *Gastroenterology* 2009; **137**: 1795–1804.
- Yuan S, Duguid WP, Agapitos D, et al. Phenotypic modulation of hamster acinar cells by culture in collagen matrix. *Exp Cell Res* 1997; **237**: 247–258.
- Scaffidi P, Misteli T, Bianchi ME. Release of chromatin protein HMGB1 by necrotic cells triggers inflammation. *Nature* 2002; **418**: 191–195.
- Al-Adsani A, Burke ZD, Eberhard D, et al. Dexamethasone treatment induces the reprogramming of pancreatic acinar cells to hepatocytes and ductal cells. *PLoS One* 2010; **5**: e13650.
- Eberhard D, O'Neill K, Burke ZD, et al. *In vitro* reprogramming of pancreatic cells to hepatocytes. *Methods Mol Biol* 2010; **636**: 285–292.
- Lee M, Chung S, Uhm DY, et al. Regulation of zymogen granule exocytosis by Ca^{2+} , cAMP, and PKC in pancreatic acinar cells. *Biochem Biophys Res Commun* 2005; **334**: 1241–1247.
- Li C, Chen X, Williams JA. Regulation of CCK-induced amylase release by PKC δ in rat pancreatic acinar cells. *Am J Physiol Gastrointest Liver Physiol* 2004; **287**: G764–771.
- Mauro LV, Grossoni VC, Urtreger AJ, et al. PKC-delta (PKC δ) promotes tumoral progression of human ductal pancreatic cancer. *Pancreas* 2011; **39**: e31–41.
- Toullec D, Pianetti P, Coste H, et al. The bisindolylmaleimide GF 109203X is a potent and selective inhibitor of protein kinase C. *J Biol Chem* 1991; **266**: 15771–15781.
- Boneh A, Mandla S, Tenenhouse HS, et al. Phorbol myristate acetate activates protein kinase C, stimulates the phosphorylation of endogenous proteins and inhibits phosphate transport in mouse renal tubules. *Biochim Biophys Acta* 1989; **1012**: 308–316.
- Ahn BK, Jeong SK, Kim HS, et al. Rottlerin, a specific inhibitor of protein kinase C δ , impedes barrier repair response by increasing intracellular free calcium. *J Invest Dermatol* 2006; **126**: 1348–1355.
- Gray MO, Karliner JS, Mochly-Rosen D. A selective ϵ -protein kinase C antagonist inhibits protection of cardiac myocytes from hypoxia-induced cell death. *J Biol Chem* 1997; **272**: 30945–30951.
- Gschwendt M, Muller HJ, Kielbassa K, et al. Rottlerin, a novel protein kinase inhibitor. *Biochem Biophys Res Commun* 1994; **199**: 93–98.
- Zhu L, Shi G, Schmidt CM, et al. Acinar cells contribute to the molecular heterogeneity of pancreatic intraepithelial neoplasia. *Am J Pathol* 2007; **171**: 263–273.
- Tian X, Jin RU, Bredemeyer AJ, et al. RAB26 and RAB3D are direct transcriptional targets of *MIST1* that regulate exocrine granule maturation. *Mol Cell Biol* 2010; **30**: 1269–1284.
- Gao N, LeLay J, Vatamaniuk MZ, et al. Dynamic regulation of *Pdx1* enhancers by *Foxa1* and *Foxa2* is essential for pancreas development. *Genes Dev* 2008; **22**: 3435–3448.

40. Furuyama K, Kawaguchi Y, Akiyama H, *et al.* Continuous cell supply from a Sox9-expressing progenitor zone in adult liver, exocrine pancreas and intestine. *Nat Genet* 2011; **43**: 34–41.
41. Kopp JL, Dubois CL, Schaffer AE, *et al.* Sox9⁺ ductal cells are multipotent progenitors throughout development but do not produce new endocrine cells in the normal or injured adult pancreas. *Development* 2011; **138**: 653–665.
42. Lin J, Fernandez I, Roy K. Development of feeder-free culture systems for generation of *ckit*⁺ *sca1*⁺ progenitors from mouse iPS cells. *Stem Cell Rev* 2011; **7**: 736–747.
43. Rooman I, De Medts N, Baeyens L, *et al.* Expression of the Notch signaling pathway and effect on exocrine cell proliferation in adult rat pancreas. *Am J Pathol* 2006; **169**: 1206–1214.
44. Molero X, Vaquero EC, Flandez M, *et al.* Gene expression dynamics after murine pancreatitis unveils novel roles for Hnf1 α in acinar cell homeostasis. *Gut* 2011; [Epub ahead of print 23 September 2011 DOI:10.1136/gutjnl-2011-300360
45. Jensen JN, Cameron E, Garay MV, *et al.* Recapitulation of elements of embryonic development in adult mouse pancreatic regeneration. *Gastroenterology* 2005; **128**: 728–741.
46. Lennerz JK, Kim SH, Oates EL, *et al.* The transcription factor MIST1 is a novel human gastric chief cell marker whose expression is lost in metaplasia, dysplasia, and carcinoma. *Am J Pathol* 2010; **177**: 1514–1533.
47. Williams JA, Sans MD, Tashiro M, *et al.* Cholecystokinin activates a variety of intracellular signal transduction mechanisms in rodent pancreatic acinar cells. *Pharmacol Toxicol* 2002; **91**: 297–303.
48. Kim JD, Seo KW, Lee EA, *et al.* A novel mouse PKC α splice variant, PKC δ IX, inhibits etoposide-induced apoptosis. *Biochem Biophys Res Commun* 2011; **410**: 177–182.
49. Xia S, Chen Z, Forman LW, *et al.* PKC δ survival signaling in cells containing an activated p21Ras protein requires PDK1. *Cell Signal* 2009; **21**: 502–508.
50. Humphries MJ, Ohm AM, Schaack J, *et al.* Tyrosine phosphorylation regulates nuclear translocation of PKC δ . *Oncogene* 2008; **27**: 3045–3053.
51. DeVries TA, Neville MC, Reyland ME. Nuclear import of PKC δ is required for apoptosis: identification of a novel nuclear import sequence. *EMBO J* 2002; **21**: 6050–6060.
52. Alahari S, Mehmood R, Johnson CL, *et al.* The absence of MIST1 leads to increased ethanol sensitivity and decreased activity of the unfolded protein response in mouse pancreatic acinar cells. *PLoS One* 2011; **6**: e28863.
53. Churchill EN, Mochly-Rosen D. The roles of PKC δ and - ϵ isoenzymes in the regulation of myocardial ischaemia/reperfusion injury. *Biochem Soc Trans* 2007; **35**: 1040–1042.

SUPPORTING INFORMATION ON THE INTERNET

The following supporting information may be found in the online version of this article:

Table S1. List of antibodies used.

Table S2. Primer sequence, annealing temperature and amplicon size for genes assessed by qRT-PCR.

Figure S1. Comparison of acinar cell differentiation in culture.

Figure S2. HMGB1 analysis in acinar cell cultures.

Figure S3. Transferrin expression in acinar cell cultures.

Figure S4. PDX1 accumulates in acinar cells only after induction of CIP.

Figure S5. Cellular localization of PKC α and ζ .

Figure S6. Inhibition of PKC δ blocks reduces cyst formation in *Mist1*^{-/-} cultures.

Figure S7. IHC for MIST1 staining in PanIN lesions.